Nanoscale

PAPER

Cite this: *Nanoscale*, 2015, **7**, 15689

Nanostructured materials detect epidermal growth factor receptor, neuron specific enolase and carcinoembryonic antigen

Raluca-Ioana Stefan-van Staden,*[a,b] Ionela Raluca Comnea-Stancu,[a,b] Carmen Cristina Surdu-Bob[c] and Marius Badulescu[c]

Received 4th July 2015,
Accepted 17th August 2015

DOI: 10.1039/c5nr04476f

www.rsc.org/nanoscale

New nanostructured materials based on thin films of Cu and Ni deposited on textile material (veil), as well as gold nanostructured microspheres were used for the design of new stochastic sensors. The stochastic sensors were able to detect simultaneously a panel of biomarkers comprising epidermal growth factor receptor, neuron specific enolase, and carcinoembryonic antigen from whole blood samples with high reliabilities – recovery tests higher than 97.00%, with a RSD (%) lower than 0.1%. The stochastic sensors had shown high sensitivities and low determination levels for the detection of the proposed panel of biomarkers making early detection of lung cancer possible by fast screening of whole blood.

Introduction

The fast quantification of chemical and biological analytes is very important for clinical diagnosis, environmental analysis, and food quality control. The demand for reliable sensors for bioanalytes in clinical laboratories has increased interest in the fabrication of economically viable sensing devices. The analytical information obtained with the sensors is directly related to the reliability of the design of sensors. Progress in sensors' technology depends on the evolution of materials. Recent progress in nanoscience and nanotechnology offers a library of functional nanomaterials with unique optical and electronic properties. These novel functional nanomaterials have potential for various applications and they are revolutionizing the multidisciplinary field of biosensors.[1,2]

Functional nanomaterials have shown that they are promising candidates in the development of sensors for the detection and quantification of bioanalytes. The remarkable characteristics of nanomaterials based on metal and metal oxide nanoparticles, ensure enhanced performance of the sensors in terms of sensitivity, selectivity, detection limit, response time, and multiplexing capability.[3] Nanomaterials like carbon nanotubes (CNTs),[4–6] graphene,[7–9] and metal/metal oxide nanoparticles like gold nanoparticles,[10–12] copper[13–15] or nickel[16–18] are promising candidates in the development of sensing platforms. The properties of these nanomaterials can be tuned according to the requirement by tailoring their shape, size, and surface structure.

Stochastic sensors are a good alternative to the classical electrochemical sensors being able to perform reliable qualitative and quantitative analyses.[19] The principle of stochastic sensors is based on channel/pore conductivity: analytes modulate ionic currents flowing through the pore into which binding sites have been engineered. The frequency of occurrence ($1/t_{on}$) of the binding events reveals the concentration of the analyte, whereas the nature of the binding events, and their duration reveals its signature; each analyte produces a characteristic signature (t_{off}),[20,21] this being influenced by its size, geometry, stereogeometry, capacity of unfolding, and velocity of passing through the channel/pore, and therefore, it is difficult to find two analytes with the same signature.[22]

In this article, new materials based on three metals: Cu, Ni, Au – engineered like thin films of copper and nickel, and gold nanostructured microspheres were used for the design of stochastic sensors. To prove the stochastic sensing capabilities of the new materials proposed we chose a panel of three lung cancer biomarkers: neuron specific enolase (NSE) and carcinoembryonic antigen (CEA) are intensively investigated due to their features for the early diagnosis and screening of cancer but also for monitoring its response to treatment or recurrence and, more recently, for the assessment of cancer risk,[23] and epidermal growth factor receptor (EGFR/HER-1) moderates the activation of a signaling pathway controlling cell proliferation, invasion, metastasis and angiogenesis.[24]

[a]*Laboratory of Electrochemistry and PATLAB Bucharest, National Institute of Research for Electrochemistry and Condensed Matter, 202 Splaiul Independentei St., Bucharest, 060021, Romania. E-mail: ralucavanstaden@gmail.com; Tel: +40751507779; Fax: +4021 3163113*
[b]*Faculty of Applied Chemistry and Materials Science, Politehnica University of Bucharest, 1-7 Polizu St., Bucharest, 011061, Romania*
[c]*Low Temperature Plasma Laboratory, National Institute for Lasers, Plasma and Radiation Physics (NILPRP), 409 Atomistilor St., Magurele, 077125, Romania*

Experimental

Reagents and materials

Epidermal growth factor receptor (EGFR/HER-1), carcinoembryonic antigen (CEA), neuron specific enolase (NSE), monosodium and disodium phosphate were purchased from Sigma Aldrich (Milwaukee, USA). Paraffin oil and NaN_3 were purchased from Fluka (Buchs, Switzerland). Engineered nanoporous 24 K gold microspheres, and thin copper and nickel nanofilms were designed by a team of NILPRP. Monosodium phosphate and disodium phosphate were used for preparation of phosphate buffer solution. Deionised water obtained from a Millipore Direct-Q 3 System (Molsheim, France) was used for the preparation of all solutions.

The standard solutions of NSE were all prepared in phosphate buffer solution (pH = 7.04). The range of concentrations was obtained by a serial dilution method from 0.125 mg mL^{-1} to 7.449 pg mL^{-1}. The standard solutions of CEA and HER-1 were prepared in saline phosphate buffer solution (pH = 7.4, with 0.1% NaN_3). A serial dilution technique was used for the preparation of solutions of CEA from 16 mg mL^{-1} to 16 pg mL^{-1}, and for HER-1 from 3.04 mg mL^{-1} to 560 pg mL^{-1}.

Instrumentation

A PGSTAT 12 potentiostat/galvanostat connected to a three-electrode cell was used for all chronoamperometric measurements, and linked to a computer *via* an Eco Chemie (Utrecht, The Netherlands) software version 4.9. The electrochemical cell was assembled with a conventional three electrode cell: the working electrode, an Ag/AgCl (0.1 mol L^{-1} KCl) as the reference electrode and a Pt counter electrode. For the pH measurements a Cyberscan PCD 6500 pH/mV-meter from Eutech Instruments was used.

Design of the sensors

The textile sensors based on Cu, and Ni nanofilms, investigated here were prepared by using a piece of nickel or copper coated textile with a length of 2.5 cm and a width of 1.0 mm connected directly to the external circuit (Fig. 1a and b).

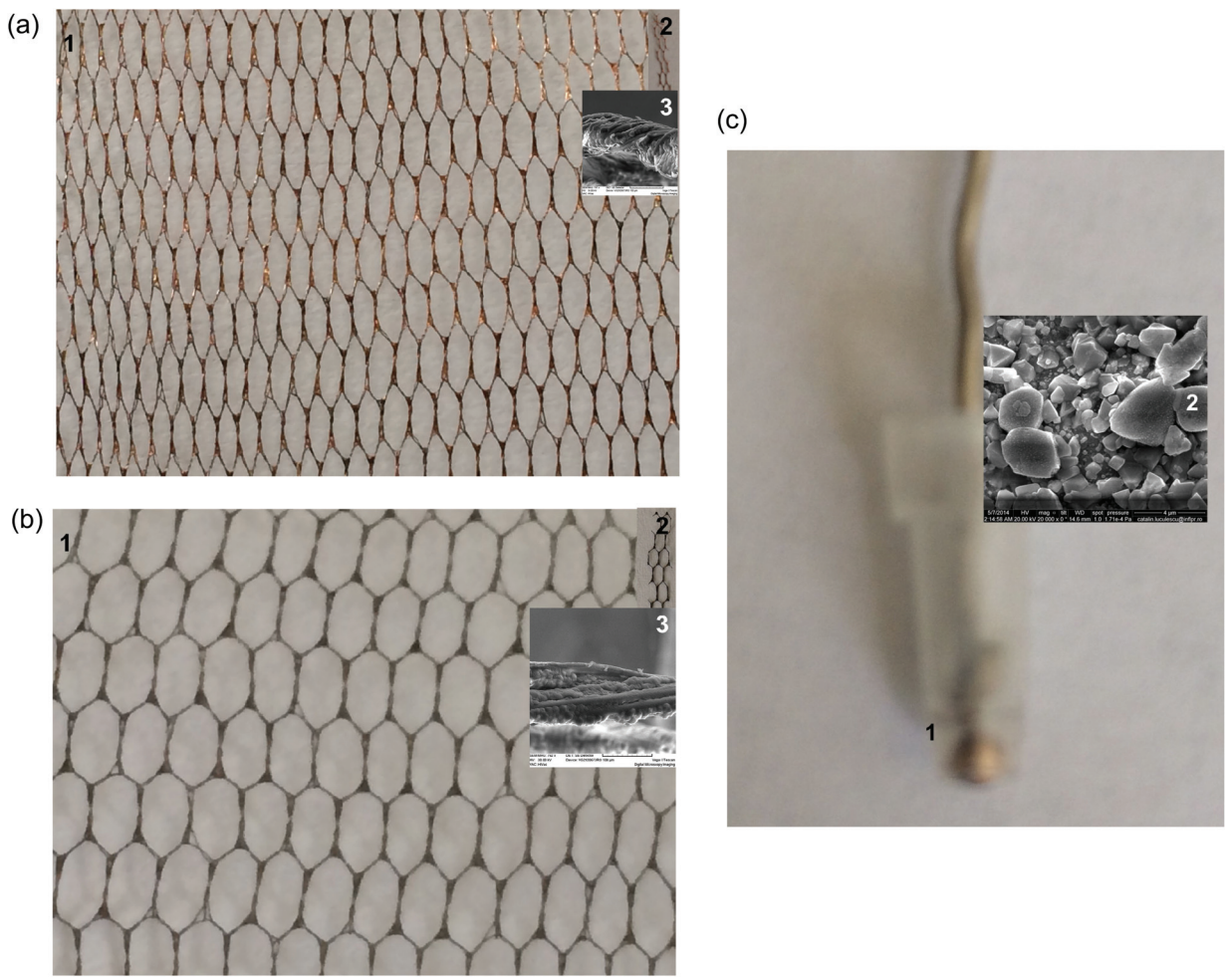

Fig. 1 Design of the sensors based on: (a) Cu nanofilm on veil – (1) bulk of veil covered with the Cu nanofilm, (2) sensor used for pattern recognition of HER-1, CEA, and NSE, (3) SEM image of the sensor; (b) Ni nanofilm on veil – (1) bulk of veil covered with the Ni nanofilm, (2) sensor used for pattern recognition of HER-1, CEA, and NSE, (3) SEM image of the sensor; (c) Au microsphere – (1) photo of the sensor setup, (2) SEM image of the surface of the Au microsphere.

One engineered nanoporous gold microsphere obtained from NILPRP of a diameter of 300 μm was fixed inside a plastic tube so that half of the sphere was outside and the other half inside the tube (Fig. 1c). A silver wire served as electrical connection to the external circuit. The active surface of the sensors was rinsed in between measurements with distilled water, and gently dried with absorbent paper.

Stochastic method

For the stochastic method, a direct chronoamperometric technique was selected for the measurements of t_{on} and t_{off} at a constant potential of 125 mV. The electrodes were dipped into a cell containing solutions of analyte of different concentrations. Values of t_{on} were read on the diagram, and the equations of calibration $1/t_{on} = f(\text{Conc.})$ for the three biomarkers were determined using statistics (linear concentration range – data obtained for t_{on} when solutions containing different concentrations of HER-1, CEA or NSE were measured using the sensors considered, the values obtained for r will help in assessing the linear concentration range, and the pair concentration $(x) - 1/t_{on}$ (y) obtained on this range will be considered to calculate the parameters of the equation of calibration using statistical methods based on the linear regression equation). Unknown concentrations of HER-1, NSE and CEA were determined by introducing the values of $1/t_{on}$ obtained after the measurements of samples in these equations of calibration.

Sample preparation

University Hospital from Bucharest provided the whole blood samples from patients who were diagnosed with lung cancer (Ethics committee approval no. 11/2013, informed consent was obtained from all subjects) in order to use them for the screening test of HER-1, NSE and CEA, and method validation. The sample volume collected for screening was 0.3 mL. These samples were collected immediately after the patients were confirmed, using the simple X-ray, with lung cancer, or after they were suspected of lung cancer. Whole blood samples from healthy patients were also provided – as negative controls. The patients were not under any treatment before collecting the samples.

The samples did not need any pre-treatment before the assay, and were analysed immediately after they were collected from the patients. The apparatus cell was filled with the whole blood sample and the unknown concentrations of the three biomarkers in whole blood samples were determined using the stochastic method described above.

Results and discussion

Response characteristics of the stochastic sensors used for the screening of HER-1, NSE and CEA

The principle of stochastic sensors is based on channel conductivity. In the absence of compounds, the channel/nanopore

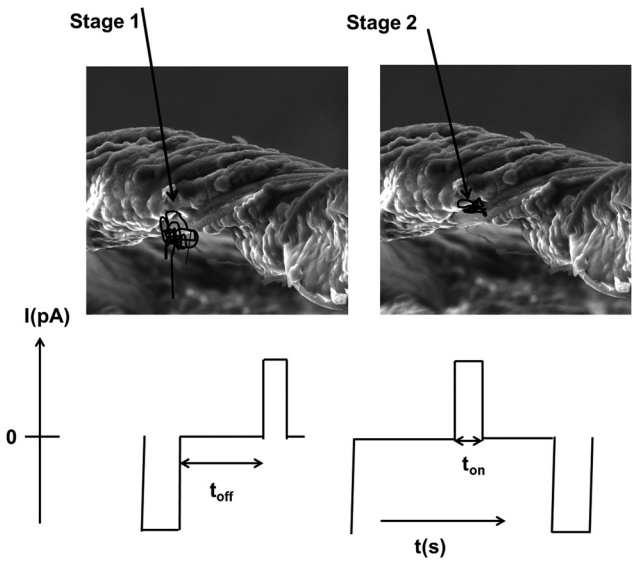

Fig. 2 Current development for stochastic sensors.

Table 1 Response characteristics of the stochastic sensors for the assay of HER-1, CEA and NSE

Stochastic sensors based on	t_{off} (s)	Linear concentration range (mg mL^{-1})	Limit of determination (mg mL^{-1})	Sensitivity (s mg^{-1} mL)	Equation of calibration
HER-1					
Cu	2	7.00×10^{-9}–1.94×10^{-7}	7.00×10^{-9}	3.45×10^{5}	$1/t_{on} = 0.009 + 3.45 \times 10^{5} \times C$; $r = 0.9983$
Ni	3.5	2.80×10^{-10}–7.00×10^{-9}	2.80×10^{-10}	4.41×10^{6}	$1/t_{on} = 0.027 + 4.41 \times 10^{6} \times C$; $r = 0.9998$
Au	1.4	2.80×10^{-10}–7.00×10^{-9}	2.80×10^{-10}	2.15×10^{6}	$1/t_{on} = 0.018 + 2.15 \times 10^{6} \times C$; $r = 0.9967$
CEA					
Cu	3.5	1.6×10^{-7}–1.6×10^{-4}	1.6×10^{-7}	4.24×10^{2}	$1/t_{on} = 0.023 + 4.24 \times 10^{2} \times C$ [a]; $r = 0.9934$
Ni	2.5	1.6×10^{-11}–1.6×10^{-8}	1.6×10^{-11}	4.30×10^{6}	$1/t_{on} = 0.026 + 4.30 \times 10^{6} \times C$ [a]; $r = 0.9950$
Au [c]	3	1.6×10^{-7}–1.6×10^{-5}	1.6×10^{-7}	2.92×10^{3}	$1/t_{on} = 0.02 + 2.92 \times 10^{3} \times C$ [a]; $r = 0.9995$
NSE					
Cu	3	1.91×10^{-6}–3.05×10^{-4}	1.91×10^{-6}	1.11×10^{3}	$1/t_{on} = 0.019 + 1.11 \times 10^{3} \times C$ [b]; $r = 0.9987$
Ni	3	7.63×10^{-6}–4.88×10^{-4}	7.63×10^{-6}	1.05×10^{2}	$1/t_{on} = 0.031 + 1.05 \times 10^{5} \times C$ [b]; $r = 0.9999$
Au	2	1.22×10^{-4}–1.95×10^{-3}	1.22×10^{-4}	8.22	$1/t_{on} = 0.034 + 8.22 \times C$ [b]; $r = 0.9950$

[a] $\langle C \rangle$ = mg mL^{-1}; $\langle t_{on} \rangle$ = s. [b] $\langle C \rangle$ = g mL^{-1}; $\langle t_{on} \rangle$ = s. [c] Ref. 25.

is always open and a constant ionic current is observed, when a certain potential is applied. In contrast, when a target molecule enters the channel/pore, it will block it, resulting in a decrease of the ionic current through the pore, and the following reactions take place:

$$Ch_{(i)} + NSE_{(i)} \Leftrightarrow Ch{\cdot}NSE_{(i)}$$

$$Ch_{(i)} + CEA_{(i)} \Leftrightarrow Ch{\cdot}CEA_{(i)}$$

$$Ch_{(i)} + HER\text{-}1_{(i)} \Leftrightarrow Ch{\cdot}HER\text{-}1_{(i)}$$

where Ch represents the channel and i the membrane-solution interface. Accordingly, the mechanism of current development takes place in two stages: the first stage when the molecule enters the channel/pore, blocking it totally or partially (the current drops to a zero value), and the second stage when the binding and redox processes take place in the channel (Fig. 2). The analytes enter the channel/pore in the order given by the following parameters: size, geometry, stereochemistry, and speed of unfolding.

The values of t_{off} represent the signatures of the analytes, and can be used for the identification of the biomarkers, while the t_{on} values were used for assessing the equation of calibration. Using the values of t_{on}, we can determine the working concentration range, the equation of calibration, sensitivity, and the limit of determination of the sensors (Table 1). Response characteristics of the stochastic sensors proposed for the screening of NSE, CEA and HER-1 are shown in Table 1. The sensors proposed for the screening of the three biomarkers designed with new materials based on films of Cu and Ni showed good response characteristics, high values of sensitivity and low limits of determination. For the assay of HER-1 the sensors based on Ni and nanoporous gold microspheres showed the best response characteristics with 280 pg mL^{-1} as the limit of determination. The sensor based on Ni proved to have good response characteristics for the assay of CEA also, with 16 pg mL^{-1}. For the assay of NSE, the lowest concentration that could be reliably determined was 7.63 μg mL^{-1} with the sensor based on Ni. The sensors were stable over a period of six months, when used daily for measurements.

The proposed stochastic sensors are also selective: different values for the signatures were obtained for the three biomarkers, but also for some other protein type of substances tested.

The sensors were used on a daily basis for more than 6 months, when the RSD (%) value of their sensitivity was less than 1.0%, proving the high stability of the proposed stochastic sensors.

Analytical applications

The proposed stochastic sensors based on thin films of Cu and Ni as well as on gold nanostructured microspheres were used for the simultaneous assay of NSE, CEA and HER-1 in whole blood samples. A qualitative assay of the three biomarkers was carried out based on their signatures (t_{off} values), and the quantitative assay was performed using the values of t_{on} (Fig. 3). The signatures (t_{off} values) of the biomarkers were identified in the diagrams recorded (Fig. 3) for blood samples. The values of t_{on} were measured and plotted in the calibration graph in order to determine the concentrations of NSE, CEA and HER-1 (Table 2). From the ten samples taken from supposed healthy patients as negative controls, in two of them were detected NSE, CEA, and HER-1 (these results were included in the table as positives); a further examination recommended by the medical doctor proved that the patients got

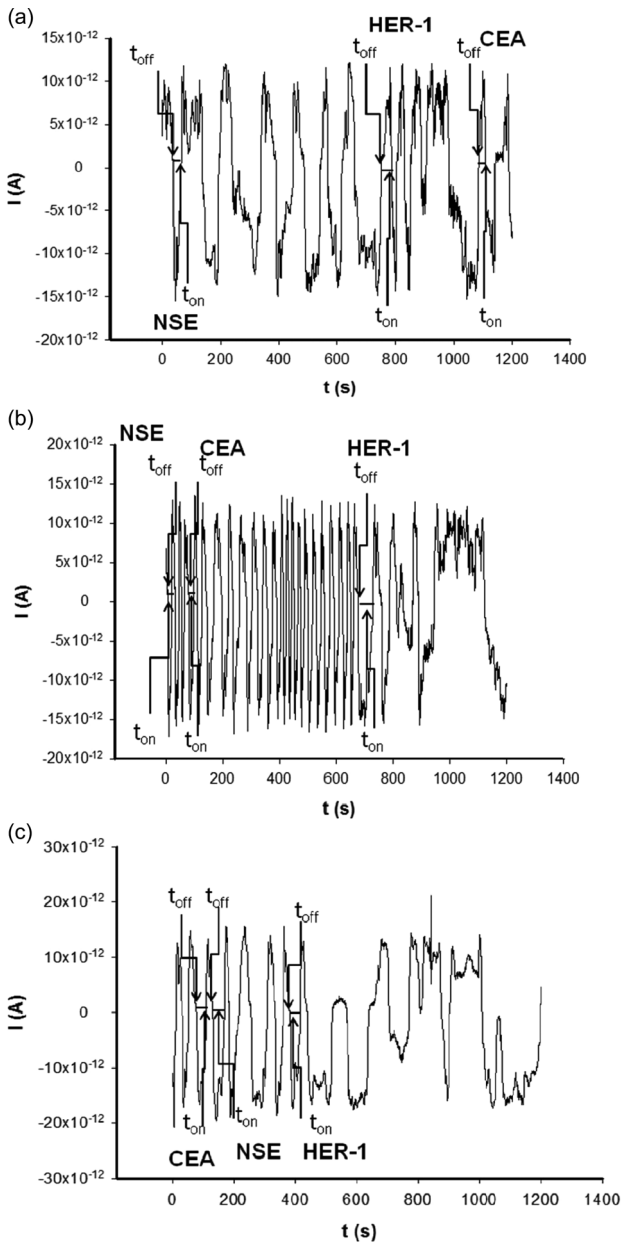

Fig. 3 Diagrams recorded for the screening of HER-1, CEA and NSE of blood samples using stochastic sensors based on: (a) Cu nanofilm on veil; (b) Ni nanofilm on veil; (c) Au microsphere.

Table 2 Analysis of NSE, CEA and HER-1 from blood samples using the stochastic sensors based on metallic ions

Sensors based on	Sample no. 1	2	3	4	5	6	7	8	9	10	*t*-test
HER-1 (pg mL^{-1})[a]											
Cu	1.53 ± 0.04	0.96 ± 0.03	1.97 ± 0.04	1.32 ± 0.04	53.00 ± 0.05	35.00 ± 0.04	94.24 ± 0.03	89.02 ± 0.04	81.05 ± 0.05	98.02 ± 0.03	3.29
Ni	1.50 ± 0.03	1.21 ± 0.03	1.18 ± 0.05	1.06 ± 0.05	57.07 ± 0.05	32.02 ± 0.03	103.03 ± 0.01	89.09 ± 0.01	89.03 ± 0.02	102.02 ± 0.02	
Au	1.72 ± 0.02	1.32 ± 0.02	1.98 ± 0.02	1.09 ± 0.05	59.09 ± 0.04	31.07 ± 0.05	96.02 ± 0.03	96.95 ± 0.03	94.24 ± 0.01	101.35 ± 0.05	
IHC	+	+	+	+	+++	++	+++	+++	+++	+++	
Bias (%)	0.15	0.21	0.25	0.17	0.32	0.35	0.47	0.52	0.50	0.43	
CEA (ng mL^{-1})[a]											
Cu	1.88 ± 0.05	170.02 ± 0.06	327.17 ± 0.06	50.15 ± 0.07	280.11 ± 0.05	405.05 ± 0.03	295.00 ± 0.03	36.02 ± 0.03	50.09 ± 0.07	315.19 ± 0.07	
Ni	1.23 ± 0.03	172.90 ± 0.03	321.07 ± 0.05	46.12 ± 0.02	276.19 ± 0.07	413.12 ± 0.07	291.98 ± 0.05	36.50 ± 0.02	52.02 ± 0.02	330.02 ± 0.08	3.42
Au	1.54 ± 0.01	170.19 ± 0.07	315.90 ± 0.07	49.02 ± 0.05	290.90 ± 0.05	405.90 ± 0.08	290.02 ± 0.08	36.20 ± 0.04	51.50 ± 0.04	323.23 ± 0.02	
ELISA	—[b]	165.00 ± 0.21	320.00 ± 0.20	50.12 ± 0.30	257.00 ± 0.67	401.20 ± 0.87	290.00 ± 0.80	35.57 ± 0.35	50.20 ± 0.30	323.00 ± 0.75	
Bias (%)	0.23	0.17	0.47	0.30	0.65	0.27	0.21	0.12	0.17	0.23	
NSE (ng mL^{-1})[a]											
Cu	98.2 ± 0.2	165.1 ± 0.2	41.4 ± 0.6	30.0 ± 0.5	44.5 ± 0.5	29.9 ± 0.2	29.1 ± 0.2	50.0 ± 0.3	75.5 ± 0.1	49.9 ± 0.1	
Ni	96.5 ± 0.2	162.2 ± 0.1	42.9 ± 0.1	33.9 ± 0.4	48.4 ± 0.3	27.8 ± 0.3	25.9 ± 0.7	52.9 ± 0.2	73.4 ± 0.2	50.0 ± 0.2	3.20
Au	93.9 ± 0.1	160.4 ± 0.3	43.0 ± 0.1	32.3 ± 0.2	40.9 ± 0.2	28.0 ± 0.1	30.0 ± 0.3	50.3 ± 0.2	71.9 ± 0.2	50.5 ± 0.3	
ELISA	92.4 ± 0.67	159.7 ± 0.9	42.0 ± 0.6	31.2 ± 0.5	37.2 ± 0.5	25.9 ± 0.7	31.0 ± 0.8	50.2 ± 0.8	70.0 ± 0.7	47.0 ± 0.5	
Bias (%)	0.13	0.23	0.17	0.15	0.28	0.17	0.31	0.14	0.15	0.12	

[a] All values are the averages of ten determinations. [b] The amount could not be determined using an ELISA kit. IHC = immunohistochemistry.

Table 3 Recovery of HER-1, CEA and NSE in whole blood samples

Sensors	Recovery[a] (%)
HER-1	
Cu	98.92 ± 0.03
Ni	98.76 ± 0.05
Au	98.98 ± 0.03
CEA	
Cu	97.52 ± 0.05
Ni	98.26 ± 0.02
Au	98.80 ± 0.03
NSE	
Cu	99.03 ± 0.05
Ni	98.99 ± 0.03
Au	99.20 ± 0.03

[a] $N = 10$.

lung cancer, at a very early stage. In the other 8 samples, no signature of CEA, NSE and HER-1 were identified in the diagrams; parallel tests were also performed for whole blood samples for CEA and NSE, and none of the two biomarkers were identified using ELISA; HER-1 was not possible to be tested from the eight patients because this analysis is available in clinical laboratories only for tumor tissue samples, and for these patients no tumor was identified using either X-Ray or PAT-CT analysis. The data shown in Table 2 proved that there is good agreement between the results obtained using the three stochastic sensors for the assay of the panel of biomarkers. Also, the paired *t*-test performed at 99.0% confidence level showed that there is no statistically significant difference between the results obtained using the proposed sensors at 99.00% confidence level, for the assay of HER-1, CEA, and NSE in whole blood samples, all values calculated being lower than the theoretical value: 4.032. The type and stage of the lung cancer could have been assessed by the medical doctor based on the results provided for the three biomarkers.

Recovery tests

Recovery tests were performed as a step of method validation. After testing the whole blood samples, a known volume of the sample was taken to which was added known concentrations of NSE, CEA and HER-1 in a ratio of 1 : 1 (v : v). The concentrations determined from the calibration graphs accordingly with the stochastic method described above, were compared with the theoretical concentrations of the spiked blood samples (Table 3). The results (Table 3) show that all three biomarkers can be reliably determined in whole blood samples, the recoveries being higher than 97.5%, with a low RSD (%) (lower than 0.1%).

Conclusions

The new nanostructured materials containing either Cu or Ni thin films deposited on textile material (veil) or gold nanostructured microparticles proved to be excellent for the design

of stochastic sensors with features of screening tests for early detection of lung cancer. The panel of biomarkers selected to be assayed simultaneously in whole blood samples comprised NSE, CEA and HER-1. The sensors were shown to be reliable for the screening of the biomarkers in whole blood samples. The main advantage of these sensors is that the samples can be used as taken from the patients, and a pre-treatment before the assay not being necessary. The sensors had great features in biomedical analysis for fast screening tests of whole blood as well as of other biological fluids like the sputum of the patients.

Acknowledgements

This work was supported by UEFISCDI PNII Program Ideas 2011–2014: PN-II-ID-PCE-2011-3-0570 and partially by PN-II-ID-PCE-2011-3-0953. Ionela Raluca Comnea-Stancu is thankful for the funding from the Sectorial Operational Programme Human Resources Development 2007–2013 of the Ministry of European Funds through the Financial Agreement POSDRU/159/1.5/S/132395.

References

1 N. J. Ronkainen, H. B. Halsal and W. R. Heineman, Electrochemical biosensors, *Chem. Soc. Rev.*, 2010, **39**, 1747–1763.
2 D. W. Kimmel, G. LeBlanc, M. E. Meschievitz and D. E. Cliffel, Electrochemical sensors and biosensors, *Anal. Chem.*, 2012, **84**, 685–707.
3 R. S. Dey, R. K. Bera and C. R. Raj, Nanomaterial-based functional scaffolds for amperometric sensing of bioanalytes, *Anal. Bioanal. Chem.*, 2013, **405**, 3431–3448.
4 Y. Wan, W. Deng, Y. Su, X. Zhu, C. Peng, H. Hu, H. Peng, S. Song and C. Fan, Carbon nanotube-based ultrasensitive multiplexing electrochemical immunosensor for cancer biomarkers, *Biosens. Bioelectron.*, 2011, **30**, 93–99.
5 G. Wang, H. Huang, B. Wang, X. Zhang and L. Wang, A supersandwich multienzyme-DNA label based electrochemical immunosensor, *Chem. Commun.*, 2012, **48**, 720–722.
6 W. Gao, H. Dong, J. Lei, H. Ji and H. Ju, Signal amplification of streptavidin-horseradish peroxidase functionalized carbon nanotubes for amperometric detection of attomolar DNA, *Chem. Commun.*, 2011, **47**, 5220–5222.
7 G. Zeng, Y. Xing, J. Gao, Z. Wang and X. Zhang, Unconventional layer-by-layer assembly of graphene multilayer films for enzyme-based glucose and maltose biosensing, *Langmuir*, 2010, **26**, 15022–15026.
8 H. Gu, Y. Yu, X. Liu, B. Ni, T. Zhou and G. Shi, Layer-by-layer self-assembly of functionalized graphene nanoplates for glucose sensing in vivo integrated with on-line microdialysis system, *Biosens. Bioelectron.*, 2012, **32**, 118–126.
9 H. Wu, J. Wang, X. Kang, C. Wang, D. Wang, J. Liu, I. A. Aksay and Y. Lin, Glucose biosensor based on immobilization of glucose oxidase in platinum nanoparticles/graphene/chitosan nanocomposite film, *Talanta*, 2009, **80**, 403–406.
10 J. C. Claussen, A. D. Franklin, A. Haque, D. M. Porterfield and T. S. Fisher, Electrochemical biosensor of nanocube-augmented carbon nanotube networks, *ACS Nano*, 2009, **3**, 37–44.
11 S. S. Kumar, K. Kwak and D. Lee, Electrochemical sensing using quantum-sized gold nanoparticles, *Anal. Chem.*, 2011, **83**, 3244–3247.
12 M. Jamal, J. Xu and K. M. Razeeb, Disposable biosensor based on immobilization of glutamate oxidase on Pt nanoparticles modified Au nanowire array electrode, *Biosens. Bioelectron.*, 2010, **26**, 1420–1424.
13 H. Pang, Q. Lu, J. Wang, Y. Li and F. Gao, Glucose assisted synthesis of copper micropuzzles and their application as nonenzymatic glucose sensors, *Chem. Commun.*, 2010, **46**, 2010–2012.
14 Q. Ghaedi, M. Montazerozohori and R. Sahraei, Comparison of the influence of nanomaterials on response properties of copper 3 selective electrodes, *J. Ind. Eng. Chem.*, 2013, **19**, 1356–1364.
15 C. Z. Li, H. X. He, A. Bogozi, J. S. Bunch and N. J. Tao, Molecular detection based on conductance quantization of nanowires, *Appl. Phys. Lett.*, 2000, **76**, 1333–1335.
16 B. Fan, Y. Feng, G. Wang, C. Zhang, A. Gu and M. Liu, A uric acid sensor based on electrodeposition of nickel hexacyanoferrate nanoparticles on an electrode modified with multiwalled carbon nanotubes, *Microchim. Acta*, 2011, **173**, 27–32.
17 K. Arshak, O. Korostynska and F. Fahim, Various structures based on nickel oxide thick films as gamma radiation sensors, *Sensors*, 2003, **3**, 176–186.
18 G. Wang, X. Lu, T. Zhai, Y. Ling, H. Wang, Y. Tong and Y. Li, Free-standing nickel oxide nanoflake arrays: synthesis and application for highly sensitive non-enzymatic glucose sensors, *Nanoscale*, 2012, **4**, 3123–3127.
19 H. Bayley and P. S. Cremer, Stochastic sensors inspired by biology, *Nature*, 2001, **413**, 226–230.
20 O. Braha, B. Walker, S. Cheley, J. J. Kasianowicz, L. Song, J. E. Gouaux and H. Bayley, Designed protein pores as components for biosensors, *Chem. Biol.*, 1997, **4**, 497–505.
21 O. Braha, L. Q. Gu, L. Zhou, X. Lu, S. Cheley and H. Bayley, Simultaneous stochastic sensing of divalent metal ions, *Nat. Biotechnol.*, 2000, **17**, 1005–1007.
22 S. Cheley, L. Q. Gu and H. Bayley, Stochastic sensing of nanomolar inositol 1,4,5-Trisphosphate with an engineered pore, *Chem. Biol.*, 2002, **9**, 829–238.
23 J. M. Ahn and J. Y. Cho, Current serum lung cancer biomarkers, *Molecular Biomarkers and Diagnosis*, 2013, **S4**, 1–7.
24 J. Mazières, W. Brugger, F. Cappuzzo, P. Middel, A. Frosch, I. Bara, G. Klingelschmitt and B. Klughammer, Evaluation of EGFR protein expression by immunohistochemistry using H-score and the magnification rule: Re-analysis of the SATURN study, *Lung Cancer*, 2013, **82**, 231–237.
25 R. I. Stefan-van Staden, I. R. Comnea-Stancu, C. C. Surdu-Bob and C. Stanciu-Gavan, Pattern recognition of neuron specific enolase and carcinoembryonic antigen in whole blood samples, *J. Mol. Recognit.*, 2015, **28**, 103–107.

